An Investigation on Uncontrolled and Vortex-Generator Controlled Supersonic Jets

PARAMESH T.[1], TAMAL JANA[2,*], MRINAL KAUSHIK[3]

[1]Department of Aerospace Engineering,
JAIN (Deemed-to-be University),
Bengaluru,
INDIA

[2]Department of Aerospace Engineering,
B.M.S. College of Engineering,
Bengaluru,
INDIA

[3]Department of Aerospace Engineering,
Indian Institute of Technology Kharagpur,
Kharagpur,
INDIA

*Corresponding Author

Abstract: - The present study is carried out with a motivation to investigate the axisymmetric supersonic jet both experimentally and computationally. An open jet facility was utilized to carry out the experiments, and the results were compared with computational simulations employing the K-omega SST turbulence model using ANSYS software. It is important to note that, the computational validation has been done incorporating the Rayleigh Pitot formula to match the centerline pressure for the uncontrolled jet, which has not been found in any other validation studies according to the authors' understanding. Besides, the experimental study is extended with a focus on evaluating the impact of Vortex Generators (VGs) on Mach 1.6 supersonic jets. The aim was to enhance jet mixing, a critical factor for improving engine performance. Various nozzle geometry modifications were explored in the past, but VGs emerged as the most effective method for optimizing jet mixing efficiency. The investigation revealed a substantial decrement in the supersonic jet core length when VGs were introduced at the nozzle exit, especially under favorable pressure gradients. This reduction in the supersonic core emphasized the role of VGs in enhancing mixing efficiency. The study also confirmed that VGs significantly distort wave patterns within the supersonic core, crucial for improved jet mixing. This research signifies the importance of VGs in augmenting the mixing of Mach 1.6 jets, offering the potential for improved jet performance and reduced noise emissions in the aerospace industry.

Key-Words: - Vortex Generator, Axisymmetric Jet, Supersonic Jet, Jet Mixing, Nozzle Pressure Ratio, Supersonic Core.

1 Introduction

High-speed supersonic jets are extensively used in the Aerospace industry. However, the supersonic jets have a limited spread or mixing with the surrounding atmospheric air compared to subsonic streams. Therefore, enhancing the mixing of a jet is critical for augmenting engine performance. This improvement is particularly important in diminishing the infrared plume and loud noise that emanates from the hot exhaust gases of the jet, [1].

Essentially, the large and small-scale vortices present inside the flow field determine the mixing rate. Note that, the larger vortices entrain a large amount of atmospheric air into the jet flow whereas the small vortices help in transporting the entrained air mass throughout the jet flow. Therefore, the right combination of large and small-scale structures is necessary to achieve good mixing. Unfortunately, the right proportion of large to small-size vortices is difficult to achieve spontaneously, [2], [3]. Hence,

Control techniques are to be used to generate the vortices in mixed proportion to achieve better mixing, [4]. The control methods can be active or passive. The Active control uses the external energy to modify the jet flow characteristics. Whereas, the passive control is achieved by the modifications in the geometry of the nozzle.

As it is known that the rate of mixing for the supersonic jet is significantly lower than that for the subsonic jet, the length of the supersonic jet is much longer when compared with the subsonic jets. The supersonic length can be found using experimental and numerical methods. The empirical relation in finding the supersonic core length for any nozzle geometry can be expressed using Equation 1, [5].

$$L_c = \left[D_h - \frac{a}{4} \right] [8.4 + 2.2\, M^2] \qquad (1)$$

To enhance the supersonic jet mixing, the passive control techniques using the geometrical modifications are very effective. For example, the notched nozzles reduce the jet noise by enveloping the sources of noise with low-speed turbulent flows [6]. On the other hand, nozzles with grooves [7], vanes [8], lobes [9], and chevrons [10], improve the jet mixing and distort the shock waves. The grooved nozzles create streamwise vortices, whereas the vanes and lobes alter shock cell structures leading to the improvement in jet mixing. Chevron nozzles are also responsible for the breakdown of the primary jet which improves the mixing and reduces the noise.

The introduction of a thin metal strip at the nozzle exit is another effective passive control method. This thin metal strip, attached at the exit of the nozzle, is known as a vortex generator (VG) or tab. The types of vortices generated depend upon the size and shape of the strip. Tab-like devices are introduced in diametrically opposite positions at the nozzle outlet, [11]. These tabs distort the development of the jet resulting in the jet splitting into two streams of high velocity. Subsequent studies also confirmed that the placement of the tabs at the nozzle lip enhances jet mixing in subsonic and supersonic flows, [12]. Particularly, the influence of tabs on augmenting the supersonic jet mixing is higher. The mixing enhancement is obtained along with noise reduction by these devices. Essentially, the centerline velocity is reduced due to the improved mixing properties of these tabs, [13]. Moreover, the streamwise vortices are created due to the tab-induced "indentation" in the shear layer, [14]. Essentially, a "trailing vortex" at the tip of tabs and a "necklace vortex" at the base of a tab are generated in this process. Later, it was observed that the cross-sectional shape of the jet changes when the vortex generators are introduced which thereby results in a higher rate of mixing, [15]. This change holds true for both subsonic, transonic, and supersonic flow conditions, suggesting a consistent underlying mechanism, independent of compressibility factors. Recent investigations have focused on various types of corrugation geometries applied to triangular or rectangular vortex generators to enhance supersonic jet mixing, [16], [17, [18].

While numerous studies have explored the influence of vortex generators on supersonic jets, there remains a gap in research specifically addressing the altered dimensions of vortex generators. Moreover, there is a need to provide the appropriate validation method since experimentally found centerline pressure data is not the actual pressure, experienced inside the jet core. Therefore, the study aims to provide an appropriate validation technique to establish a reliable computational model while matching the experimental results. Moreover, the study is extended to understand the effect of a pair of vortex generators positioned 180° apart at the exit of a Mach 1.6 axisymmetric nozzle, considering varied jet expansion states. By adjusting the nozzle pressure ratio (NPR) from 2.5 to 6 in steps of 1.75, different levels of expansion at the nozzle outlet are simulated. This research comprises three primary phases. Initially, the reduction in the supersonic core length is measured by evaluating the total pressure decay along the jet's centerline due to the vortex generators. Secondly, the jet spread both in line with and perpendicular to the vortex generators is investigated by analyzing pressure profiles. Furthermore, the impact of the vortex generators on the supersonic core length is qualitatively assessed utilizing the Schlieren image visualization technique.

2 Methodology

The experiments have been conducted utilizing an open jet test facility at the Global Academy of Technology, Bengaluru. The primary objective is to investigate the behavior of a Mach 1.6 jet. Based on the Area-Mach number relationship, the convergent divergent nozzle was designed to have a jet of 1.6 Mach number. According to the air storage capacity and the mass flow rate of the air, the ideal diameter of the throat of the nozzle was chosen as 9 mm and the inlet and exit diameters were considered as 20 mm, and 10.06 mm, respectively. The 32 mm outer periphery of the nozzle was chosen to ensure a good

fit and alignment within the settling chamber's flange. The designed Nozzle can be found in Figure 1.
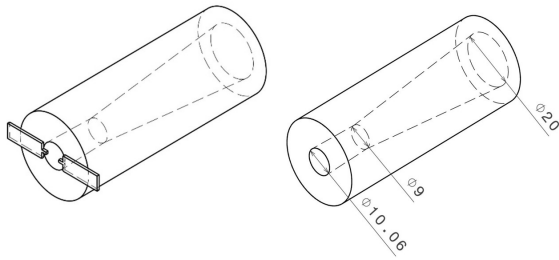

Fig. 1: CD Nozzle design with the dimensions

This study aims to investigate the jet flow characteristics of overexpanded, correctly expanded, and underexpanded states, where the jets are ejected from the nozzle designed for a Mach 1.6 flow. The settling chamber pressure corresponding to the correct expansion case has been set to 4.25 Bar. To explore the varied conditions from over-expanded to under-expanded, the air is supplied at different nozzle pressure ratios (NPR). NPR signifies the ratio of the total pressure at the settling chamber to the atmospheric pressure at the nozzle exit. Experiments are conducted for over-expansion at NPR 2.5, correct expansion at NPR 4.25, and under-expansion at NPR 6.

Vortex generators, which are small metal strips about 1 millimeter thick, are positioned at opposite ends of the nozzle exit. These generators, designed to cover 5 percent of the total nozzle exit area, were crafted with an aspect ratio of 2, meaning the length is twice that of the width.

The aluminum Pitot probe, with an outer diameter of 0.6 mm and an inner diameter of 0.4 mm, is instrumental in measuring pressure within the supersonic jet flow. When the supersonic jet encounters the Pitot probe, it generates a bow shock ahead of the probe inlet. The Pitot tube is capable of measuring total pressure behind the bow shock wave (P_{02}) in a supersonic flow, as well as the stagnation pressure of a subsonic flow. The total pressure of the jet ahead of the shock wave (P_{01}) can also be determined using the normal shock relations, as expressed by Equation 2, [19].

$$\frac{P_{o2}}{P_{o1}} = \left(1 + \frac{2\gamma}{\gamma+1}(M_1^2 - 1)\right)^{\frac{-1}{\gamma-1}} \left(\frac{(\gamma+1) M_1^2}{(\gamma-1) M_1^2 + 2}\right)^{\frac{\gamma}{\gamma-1}} \quad (2)$$

Where M_1 is the incoming supersonic freestream Mach number.

Essentially, the Pitot pressure is the total pressure of the jet flow measured behind the bow shock

formed due to the insertion of the Pitot tube into the flow field. To record the pressure values, the Pitot tube is connected to the pressure scanner through a PVC tube. The accuracy of the pressure scanner is +0.01 bar. A software-controlled 3-axis traverse mechanism is used to position the Pitot tube accurately within the jet flow.

The measured Pitot pressure (P) is non-dimensionalized by the settling chamber pressure (Po). Also, the distance in the jet flow axis (X) and the perpendicular axes (Y and Z) are made non-dimensional by the exit diameter (De) of the nozzle. The primary objective of the research is to assess the impact of vortex generators on understanding and controlling the mixing characteristics of the Mach 1.6 jet. For a detailed investigation into the characteristics of the Mach 1.6 jet flow, the flow visualization method known as the Schlieren technique is utilized to capture the wave patterns in the jet flows.

In understanding the flow characteristics of a Mach 1.6 jet, the utilization of a Computational model aids in simulating the jet's behavior, predicting flow patterns, and quantifying various parameters without requiring extensive physical testing. Employing commercially available software like ANSYS enables the analysis of the jet for understanding flow structures and characteristics. Based on the experimental observation to study the inherent flow physics of supersonic axisymmetric jet. Therefore, the Computational model is developed to study the characteristics of a Mach 1.6 jet. The 3-D nozzle and atmospheric domain are created using CATIA v5 software as shown in Figure 2. The CD Nozzle is designed with the same dimensions as mentioned above in Figure 1. Based on the existing literature [20], the jet spread domain extends up to 30 times the exit diameter, and the atmospheric domain length is chosen as 30 times the exit diameter of the Nozzle for the study. This design plays a crucial role as it serves as the fundamental framework for subsequent simulations and analysis.
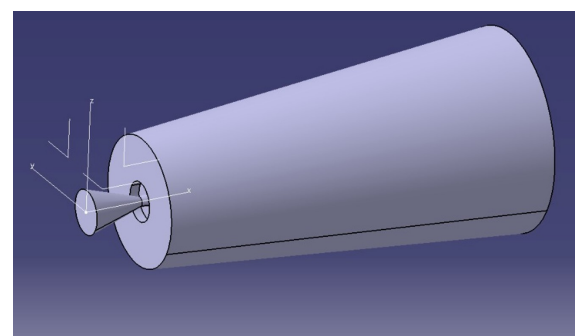

Fig. 2: Design of nozzle with far-field in CATIA V5

Following the design phase, the model is imported to ICEM CFD to develop a mesh. Meshing is vital in CFD simulations as it divides the model into smaller elements for accurate calculations. Part names are assigned in the model and a blocking technique is used to create an appropriate mesh structure. In the current investigation, the computational model has been discretized using a structural hexahedral mesh as shown in Figure 3, resulting in 2 million elements after a grid independence study, facilitating the necessary detail for precise analysis. The mesh skewness is maintained at about 0.5, ensuring a regular grid of ideal geometrical shape and establishing a node-to-node connection for a more seamless simulation. The y+ value in the near-wall zone is maintained within the range of 5 to 30. Additionally, the mesh demonstrates a variation of approximately 5 to 10 μm in spacing in the near-wall region, satisfying the y+ value near the wall. This modification is intended to ensure that the mesh near the jet's centerline, spanning from the nozzle inlet to the enclosure's end downstream, is extremely fine. This finely detailed mesh in this specific region aids in capturing shocks efficiently, thereby enhancing the computational efficiency of the investigation.
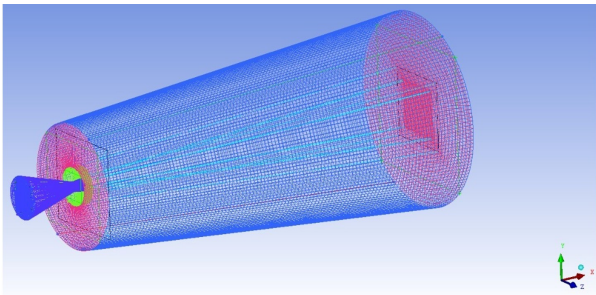
Fig. 3: Mesh model in ICEM-CFD

The numerical simulation is performed using Reynolds Averaged Navier Stokes (RANS) equations with the Shear Stress Transport (SST) κ−omega turbulence model. The turbulence equation consists of the equation for the kinetic energy (κ) and specific dissipation rate (ω).

The equation for kinetic energy and specific dissipation rate are provided in Equation 3 and Equation 4, respectively.

$$\frac{\partial}{\partial t}(\rho k) + \frac{\partial}{\partial x_i}(\rho k u_i) = \frac{\partial}{\partial x_j}\left(\alpha_k \frac{\partial k}{\partial x_j}\right) + G_k - T_k + S_k \tag{3}$$

$$\frac{\partial}{\partial t}(\rho \omega) + \frac{\partial}{\partial x_i}(\rho \omega u_i) = \frac{\partial}{\partial x_j}\left(\alpha_\omega \frac{\partial \omega}{\partial x_j}\right) + G_\omega - T_\omega + D_\omega + S_\omega \tag{4}$$

T_k and T_w are the dissipation of k and ω due to turbulence, respectively. S_k and S_ω are the source terms.

The (SST) κ−omega turbulence model was employed to effectively capture the complex viscous and compressibility effects occurring within the flow. Notably, the (SST) κ−omega model accounts for dilatation dissipation seen in high Mach-number flows, a phenomenon caused by compressibility that is not present in incompressible flows. The choice of the (SST) κ−omega model was determined by the necessity to simultaneously address high turbulence flow and low Reynolds number effects in high Mach-number flow conditions.

Table 1 shows the detailed boundary conditions imposed on the simulation model. These include parameters such as nozzle inlet pressure, wall conditions, far-field and near-field settings, atmospheric domain, and specifics related to the turbulence model used. The boundary conditions outlined in Table 1 were crucial in setting the guidelines for the simulation and were accurately replicated within the CFX software, as indicated in Figure 4.

Table 1. Boundary conditions for the numerical model

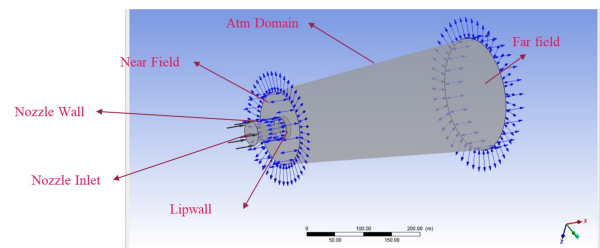| Boundary conditions	
Nozzle inlet	Pressure Inlet (3,5,7 bar)
Nozzle wall	Wall
Far-field	
Near Field	Opening - 1 atm
Atmospheric domain	
Lip wall	Wall

Fig. 4: Assigned boundary conditions in CFX

Due to the axisymmetric nature of the flow, a planar contour was chosen to comprehend the physics behind the flow and the formation of shock cells.

For the numerical model, in the supersonic flow regime, the total pressure behind the bow shock

along the jet centerline is obtained by substituting the corresponding values of Mach number and static pressure, ahead of the shock, along the centerline in the Reyleigh Pitot formula, as given by Equation 5, [21].

$$\frac{P_{o2}}{P_1} = \left(\frac{(\gamma+1)^2 \, M_1{}^2}{4\gamma M_1{}^2 - 2(\gamma-1)}\right)^{\left(\frac{\gamma}{\gamma-1}\right)} \left(\frac{1-\gamma+2\gamma \, M_1{}^2}{\gamma+1}\right) \quad (5)$$

Where P_{02} is the total pressure behind the normal shock. P_1 is the freestream static pressure. M_1 is the incoming supersonic freestream Mach number.

The total pressures for supersonic and subsonic cases are made dimensionless to obtain p/p_o. The obtained values from the computational model are compared with experimental data which confirms that the CFD model data is in proximity with the experimental data, as can be seen in Figure 5 and Figure 6. It is important to note that, the centerline pressure plot for the experimental and the numerical observation cannot be directly compared as the supersonic core is wave-dominated and the pitot probe essentially measures the pressure behind the bow shock. Since the supersonic core is wave-dominated, there is no way for the experimental intrusive pressure measurement technique to measure the actual total pressure experienced in the supersonic core. Therefore, the Rayleigh Pitot formula is utilized to convert the static centerline pressure (computationally calculated) to the total pressure downstream of the bow shock. Essentially, the calculated total pressure downstream of the bow shock from the computational data is compared to the experimental measured total centerline pressure, as shown in Figure 5.

The efficacy of the numerical model was also tested by comparing its results with experimental Schlieren image and Numerical CFD particularly focusing on the Mach disk formation at NPR 6. The comparison between the Schlieren and the numerical CFD data, as shown in Figure 6, demonstrates that the numerical model is in line with the experimental results, particularly regarding shock core length.
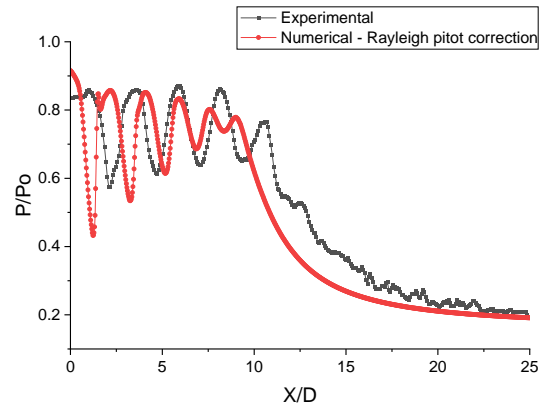
Fig. 5: Comparison of centreline total pressure ratio for experimental and computational axisymmetric uncontrolled Mach 1.6 jet at NPR 6
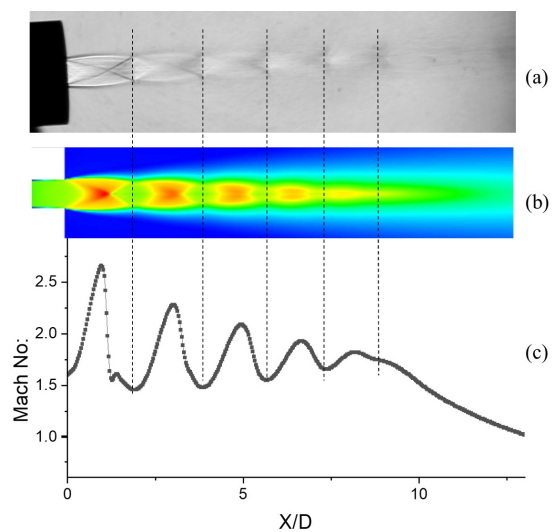
Fig. 6: (a) Schlieren image, (b) computational Mach contour, (c) Mach number vs X/D plot for the uncontrolled axisymmetric jet at NPR 6

3 Results and Analysis

In the domain of jet studies, the decay in centerline pressure is a critical parameter that provides insights into the propagation and mixing of a jet. It essentially measures how fast the mixing process occurs within the jet's flow field. A more rapid decline in centerline pressure indicates that the jet mixing is more efficient. Additionally, centerline pressure decay helps defining the boundaries of the jet core, which essentially refers to the region along the jet's axis where the supersonic jet remains dominant. It can be noted that the effectiveness of the vortex generators is measured by the rate of decrease in the potential core region of the jet.

3.1 Uncontrolled Jet

The peak and trough of the centerline pressure decay (Figure 7) show the region of the supersonic core in the supersonic jet. The centerline pressure along the Y axis is non-dimensionalized by the settling chamber pressure and the axial length along the X axis is non-dimensionalized by the exit diameter of the axisymmetric jet. It is easy to observe that, for the uncontrolled Mach 1.6 jet, the supersonic core prevails around X/D=12, and after that, there is a characteristics decay region.
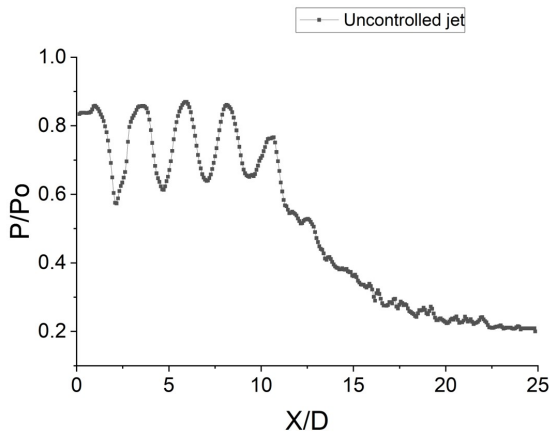

Fig. 7: Centerline pressure decay for the axisymmetric uncontrolled jet at NPR 6

Schlieren visualization, a widely utilized optical method, demonstrates the fluid flow variations based on density gradients. Strong expansion waves, Mach Disc, region of subsonic flow, oblique shock, and shock cell length can be seen in Figure 8 and Figure 9 revealing a significant presence of barrel shock structures within the jet core.
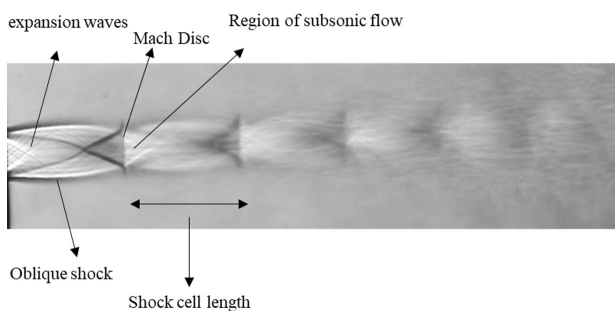
Fig. 8: Schlieren image for the axisymmetric uncontrolled jet at NPR 6
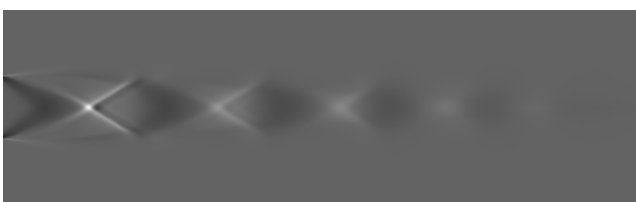
Fig. 9: Density gradient for the axisymmetric uncontrolled jet at NPR 6 (computational data)
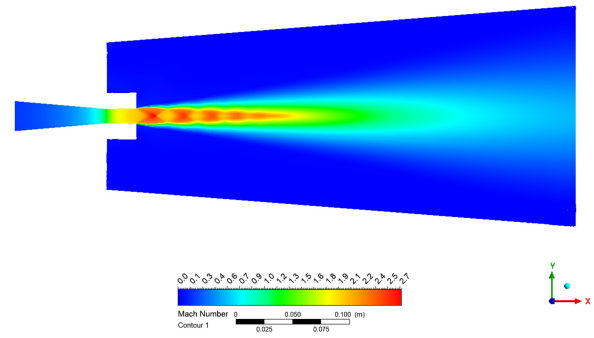
Fig. 10: Mach contour of the axisymmetric uncontrolled jet at NPR 6 (computational data)
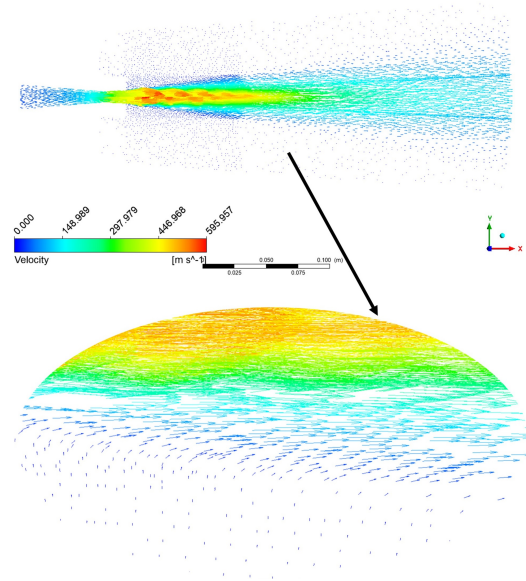
Fig. 11: Velocity vectors of the axisymmetric uncontrolled jet at NPR 6 (computational data)

The Mach contour, displayed in Figure 10, offers insight into the velocity distribution within the axisymmetric supersonic jet designed for a Mach number of 1.6. In Figure 11, the velocity vectors of the streamlines are depicted, revealing the process of entrainment, where atmospheric air is drawn into the jet flow and the subsequent mixing is obtained between the entrained air and the core jet flow.
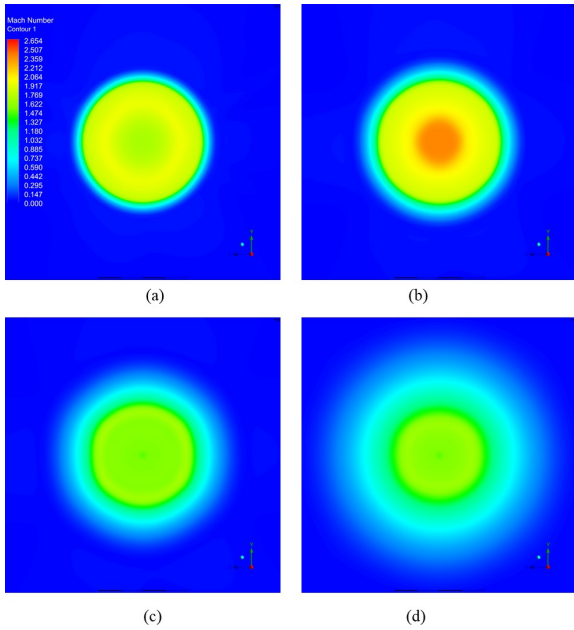
Fig. 12: Radial Mach contour for the axisymmetric uncontrolled jet at NPR 6 (a) at x = 0.5D_e, (b) at x = 1D_e, (c) at x = 2D_e, (d) at x = 4D_e (computational data)
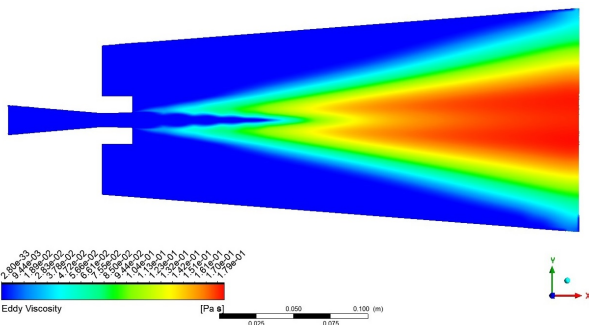
Fig. 13: Eddy viscosity contour for the axisymmetric uncontrolled jet at NPR 6 (computational data)
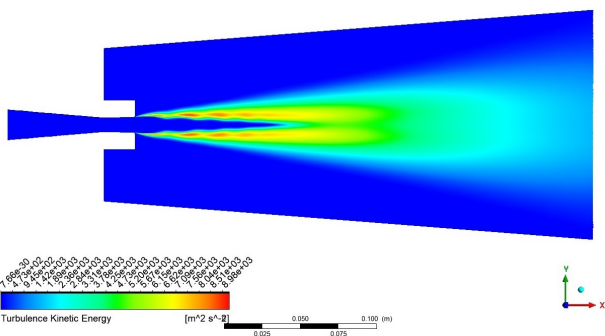

Fig. 14: Turbulence kinetic energy contour for the axisymmetric uncontrolled jet at NPR 6 (computational data)

Figure 12 illustrates the radial distribution of Mach numbers in an axisymmetric uncontrolled jet, specifically for a nozzle pressure ratio (NPR) of 6.

The radial Mach contour provides a visual representation of how the Mach number varies across different radial positions from the centerline of the jet. It is interesting to observe that the centerline velocity is maximum at x=1D_e and the radial fluctuation in velocity distribution is lesser towards the downstream direction.

Eddy viscosity in supersonic jet mixing signifies the apparent viscosity accounting for turbulent fluctuations, influencing momentum transport. Figure 13 is the Contour of Eddy viscosity for the uncontrolled Jet at NPR 6. This parameter is particularly significant as it facilitates the understanding of how momentum and energy are transported within the turbulent flow, offering insights into the spreading and entrainment of the jet into the surrounding air. On the other hand, turbulent kinetic energy represents the energy associated with the turbulent fluctuations within the flow field. It is crucial for assessing the strength of the turbulent structures within the jet, providing valuable information about the mixing characteristics of the jet with the ambient atmosphere. Higher values indicate a more energetic, turbulent flow, influencing the dispersion and dissipation of the jet into the surrounding air. The Eddy viscosity and turbulent kinetic energy in the near stream region are observed to be higher at the shear layer of the jet where the mixing happens vigorously (Figure 13 and Figure 14]. Essentially, higher eddy viscosity and turbulent energy at the free shear layer are responsible for higher mixing at that region. As the jet spreading is eventually accomplished at far downstream, the intensity of eddy viscosity and turbulent kinetic energy are seen to be uniform at the far downstream region.

3.2 Vortex Generator Controlled Supersonic Jet

The changes in centerline pressure for both uncontrolled and controlled jets for the underexpansion condition, which corresponds to NPR 6, are examined using centerline pressure distribution, as shown in Figure 15. When looking at the uncontrolled jet, one can observe the supersonic core of the jet extends up to an axial distance of approximately X/D = 13. However, by introducing vortex generators at the nozzle exit, the length of the jet's core is significantly reduced to about X/D = 4. The core length reduction is expressed in terms of percentage, calculated using Equation 6.

Percentage Reduction in core length (ΔL) =
$$\frac{L_{uncontrolled\ jet} - L_{controlled\ jet}}{L_{uncontrolled\ jet}} \times 100 \qquad (6)$$
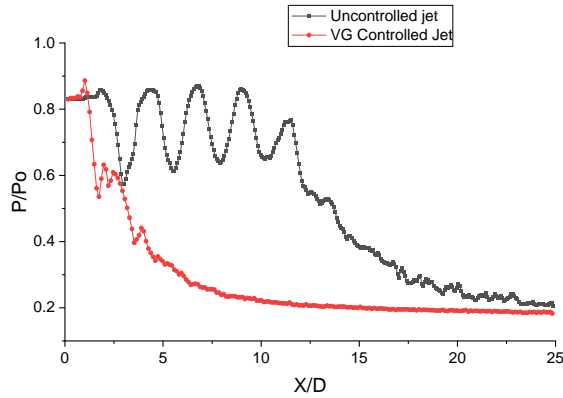
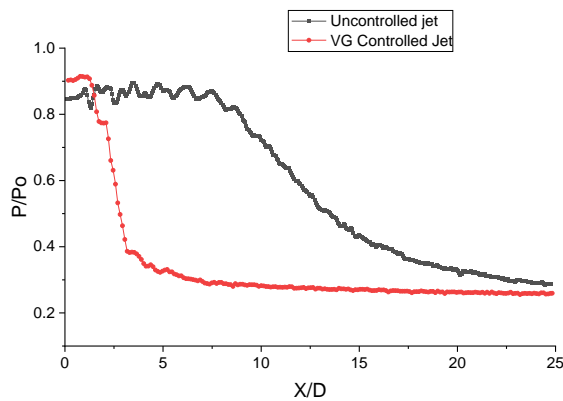Fig. 15: Pressure decay along the centerline of the jet at NPR 6

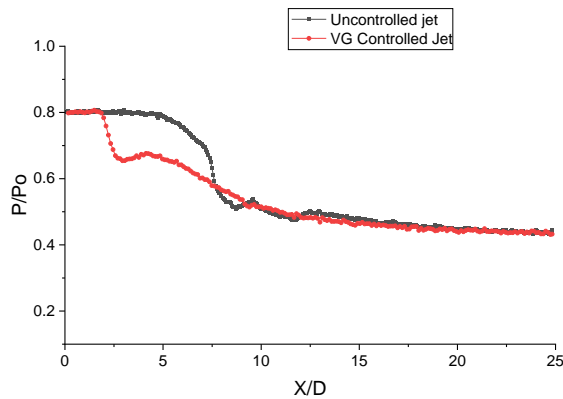Fig. 16: Pressure decay along centerline of jet at NPR 4.25

Fig. 17: Pressure decay along the centerline of the jet at NPR 2.5

This reduction corresponds to a remarkable decrease of around 69.23% in the core length. The introduction of uniformly sized small-scale vortical structures into the jet field is the primary reason behind this enhanced mixing. Notably, it is observed that uncontrolled jets attain a self-similar profile beyond $X/D = 24$, while controlled jets achieve self-similarity beyond $X/D = 10$.

Transitioning to NPR 4.25, which corresponds to a correct expansion level, as depicted in Figure 16, the decay in centerline pressure for both uncontrolled and controlled jets exhibits a similar trend. In this scenario, the controlled jet with rectangular tabs at the nozzle exit significantly outperforms the uncontrolled jet, resulting in an impressive core length reduction of approximately 66.6%. Also, it is observed that uncontrolled jets attain a self-similar profile beyond $X/D = 23$, while controlled jets achieve self-similarity beyond $X/D = 6$. This suggests that early viscous effects play a dominant role in the performance of controlled jets.

Figure 17 portrays the decay in centerline pressure at NPR 2.5, which is characterized by an overexpanded state. Here, the controlled jet demonstrates a core length reduction of approximately 33.33% compared to the uncontrolled jet. Also, we've noticed that uncontrolled jets keep a self-similar pattern beyond $X/D = 12.5$, while controlled and uncontrolled jets reach this point slightly sooner, at $X/D = 11.5$.

These observations collectively demonstrate the efficiency of promoting enhanced mixing through the use of vortex generators placed at the nozzle exit for a Mach 1.6 circular nozzle. The highest level of mixing is achieved in the overexpanded condition (NPR 6), resulting in a core length reduction of up to 69.23%. Vortex generators are particularly effective in this state due to their ability to shed uniform-sized vortices in the presence of an adverse pressure gradient. The study also quantifies the percentage reduction in core length for different NPRs, confirming the best expansion condition that leads to maximum mixing. The results suggest that the vortex generator performs better in underexpanded conditions with favorable pressure gradients.
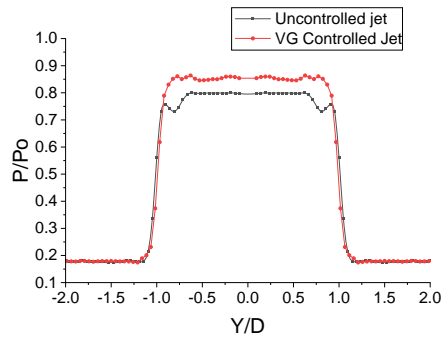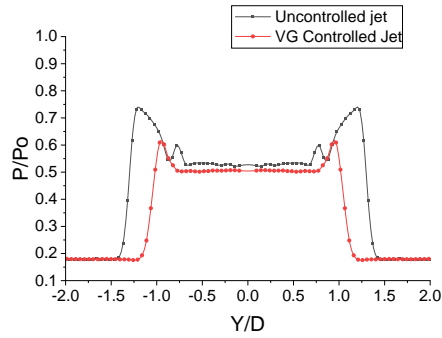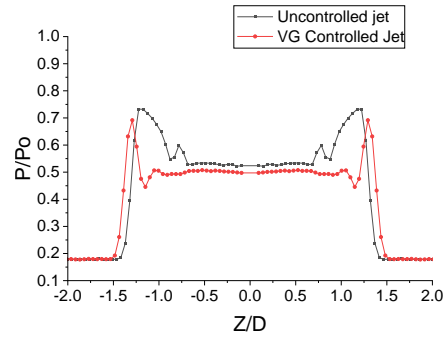
Y Profile - along the vortex generator   Z Profile - perpendicular to the vortex generator
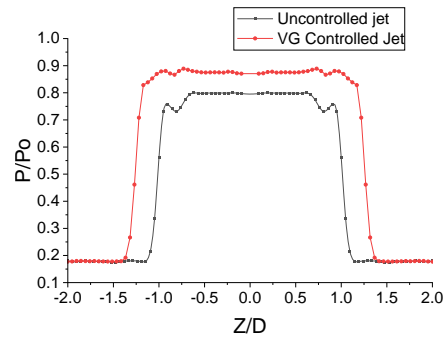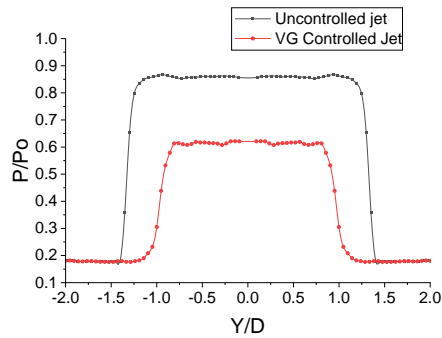
a)   X/D = 0.5
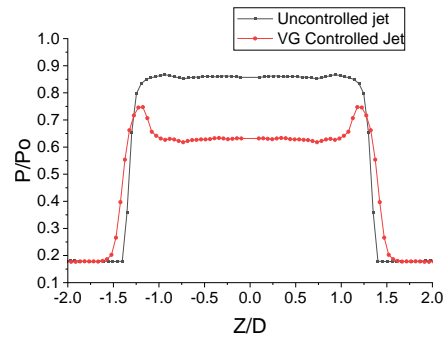
Y Profile - along the vortex generator   Z Profile - perpendicular to the vortex generator
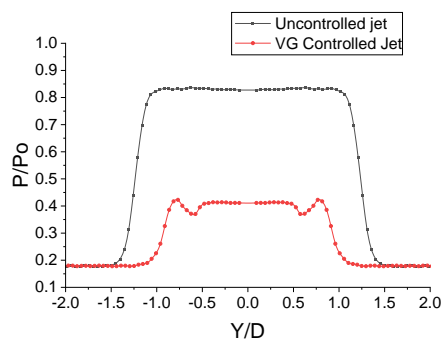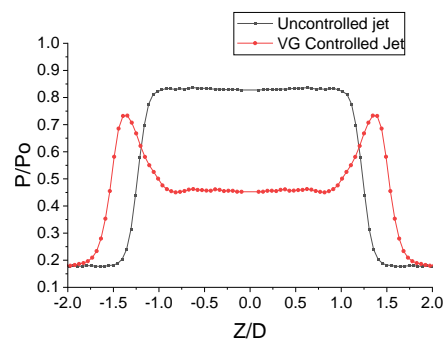
b)   X/D = 1

Y Profile - along the vortex generator   Z Profile - perpendicular to the vortex generator
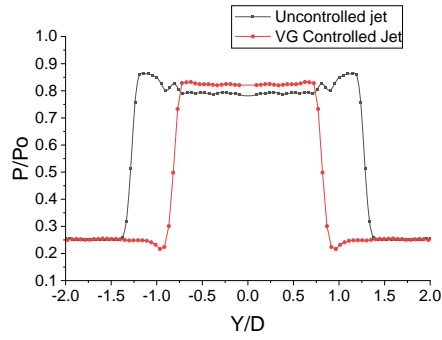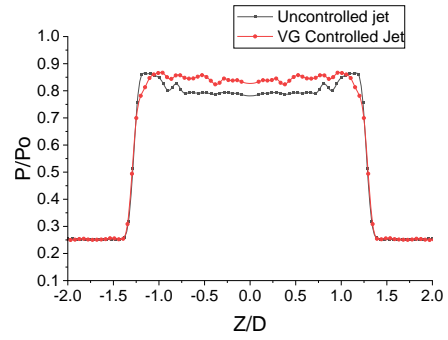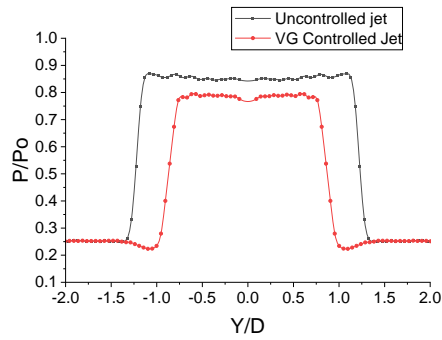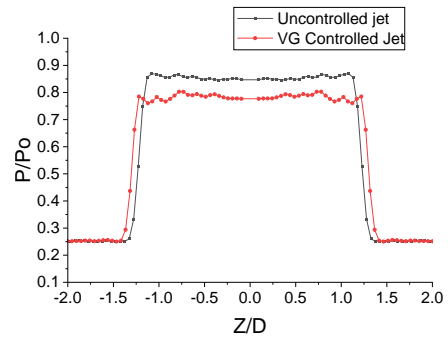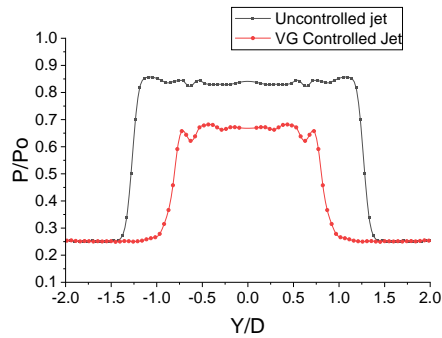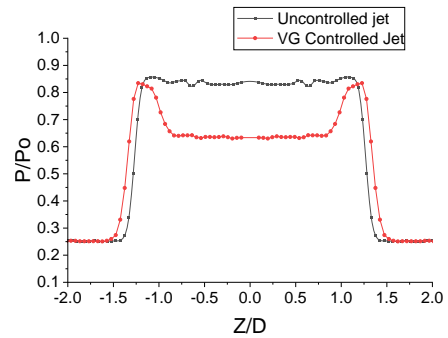
c)   X/D = 2

Y Profile - along the vortex generator   Z Profile - perpendicular to the vortex generator

d)   X/D = 4

Fig. 18: Pressure distributions for uncontrolled and VG-controlled jets at NPR 6

Fig. 19: Pressure distributions for uncontrolled, VG-controlled jets at NPR 4.25

Y Profile - along the vortex generator

Z Profile - perpendicular to the vortex generator

a)   X/D = 0.5

Y Profile - along the vortex generator

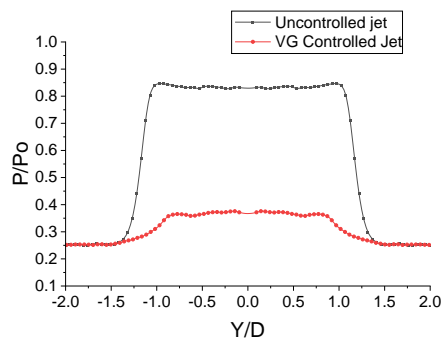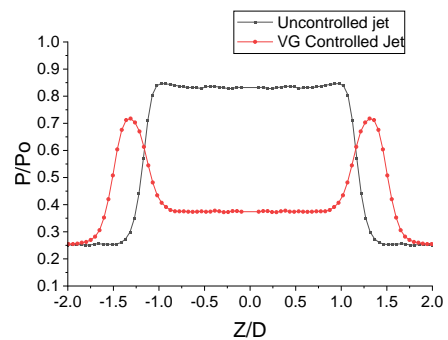Z Profile - perpendicular to the vortex generator

b)   X/D = 1

Y Profile - along the vortex generator

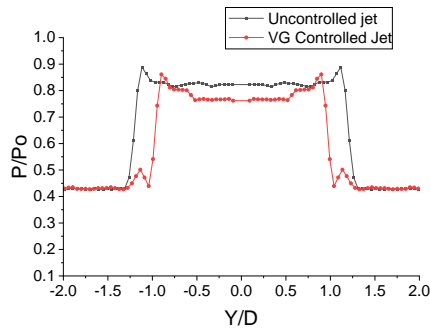Z Profile - perpendicular to the vortex generator
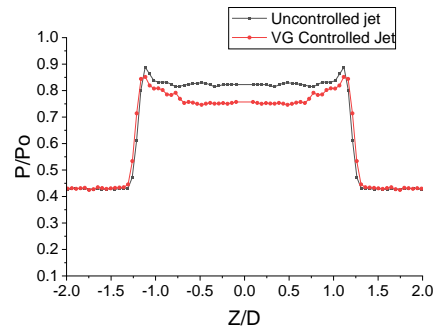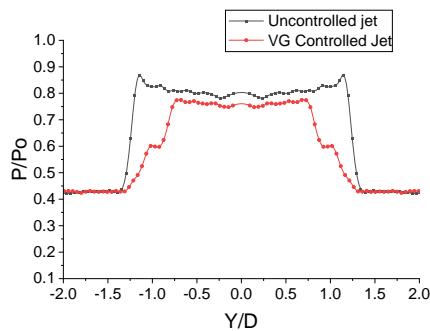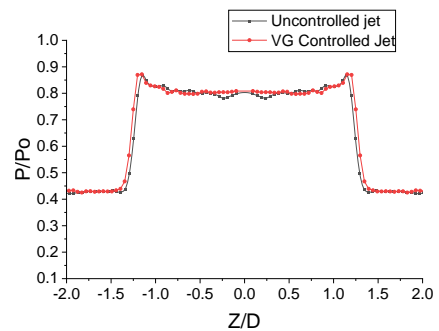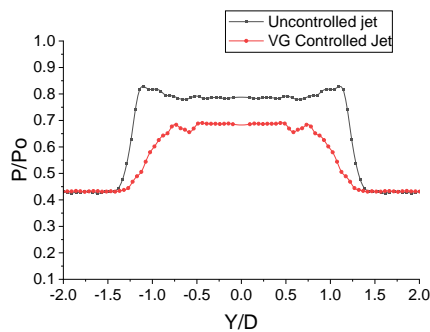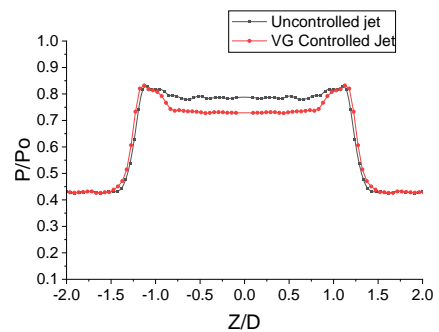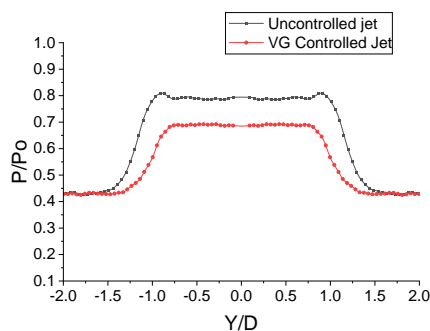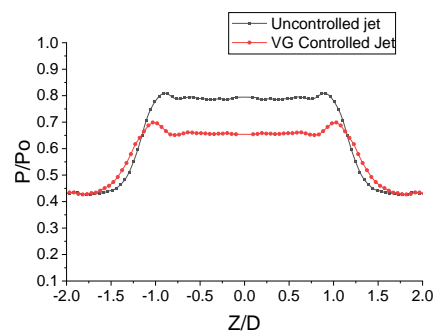
c)   X/D = 2

Y Profile - along the vortex generator

Z Profile - perpendicular to the vortex generator

d)   X/D = 4

Fig. 20: Pressure distributions for uncontrolled, VG-controlled jets at NPR 2.5

The study explored the pressure changes along the length and width of the plain rectangular tabs at different streamwise positions across various NPR sets. The study involved plotting the non-dimensional total pressure against the non-dimensional distance along the tab length (Y/D) and tab-width (Z/D) for varying axial positions. The radial pressure profiles for controlled and uncontrolled jets along the VG and Normal to VG are illustrated in Figure 18, Figure19 and Figure20 respectively. Figure 18 depicts the pressure profiles for controlled and uncontrolled jets at NPR 6 for axial positions of X/D = 0.5, 1, 2, and 4 along the VG and normal to the VG. Similarly, pressure plots have been presented for NPR 4.25 and 2.5 as shown in Figure 19 and Figure 20, respectively.

The primary concern regarding VG-induced controlled jets is flow asymmetry. It's critical to ensure that the control method doesn't introduce significant asymmetry while enhancing mixing. To explore this, pressure distributions along and across the VGs were measured, focusing on controlled jets' impact concerning free jets.

For underexpansion (NPR 6), introducing the VGs sheds more vortices closer to the jet axis. At X = 0.5D, pressure profiles show considerable oscillations, due to the relaxation effect caused by jet injection into a larger environment. As the distance increases, oscillations diminish. For the NPR 6, 4.25, and 2.5, the jet spread is reduced along the vortex generator and enhanced in the direction normal to the vortex generator leading to effective mixing leading to large reduction in the pressure ratio.

The pressure profile reveals two distinct peaks in the radial profile, illustrating two separate jet streams. Jet spread perpendicular to the VG orientation is higher due to counter-rotating streamwise vortices generated by the VG. This inward entrainment of the surrounding flow towards the core and outward ejection of the core flow introduces additional jet spreading perpendicular to the VG orientation.

Essentially, the VG introduces small-scale mixed-size vortices, beneficial for mixing. It can be noted that the interaction among the mixed-size vortices re-establishes symmetry in the flow field. VG shows maximum spread and improved symmetry in the jet flow field.
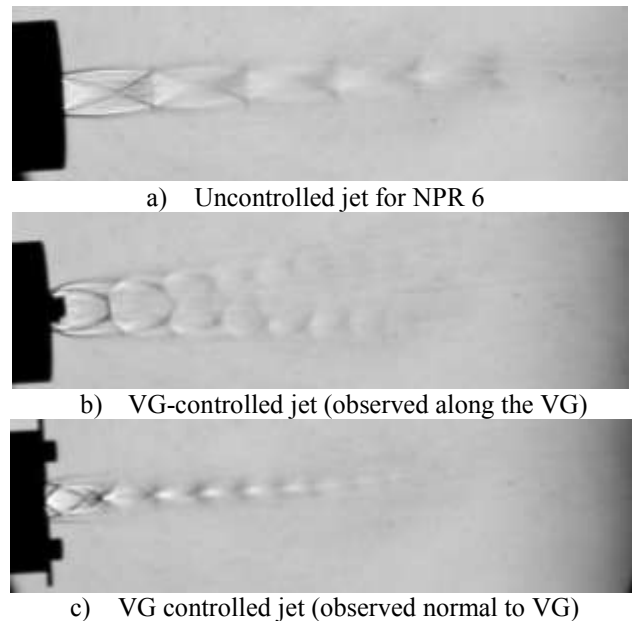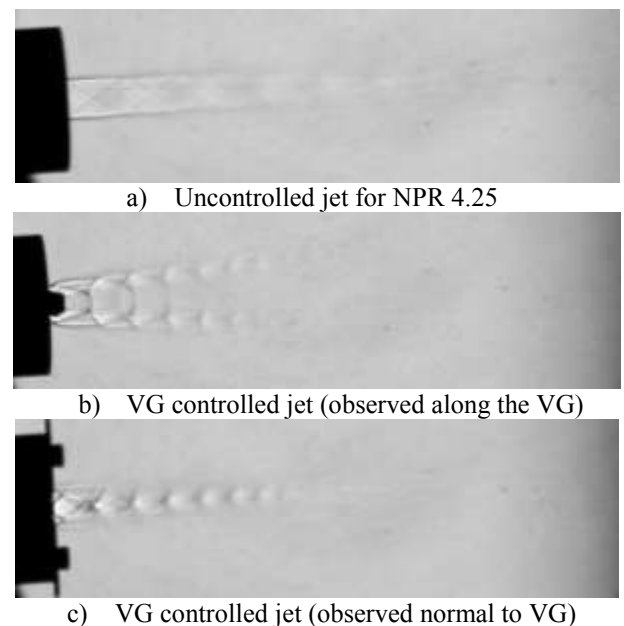
a)   Uncontrolled jet for NPR 6

b)   VG-controlled jet (observed along the VG)

c)   VG controlled jet (observed normal to VG)

Fig. 21: Schlieren images of uncontrolled and VG-controlled jets at NPR 6

a)   Uncontrolled jet for NPR 4.25

b)   VG controlled jet (observed along the VG)

c)   VG controlled jet (observed normal to VG)

Fig. 22: Schlieren images of uncontrolled and VG controlled jets at NPR 4.25

a)   Uncontrolled jet for NPR 2.5

b)   VG controlled jet (observed along the VG)
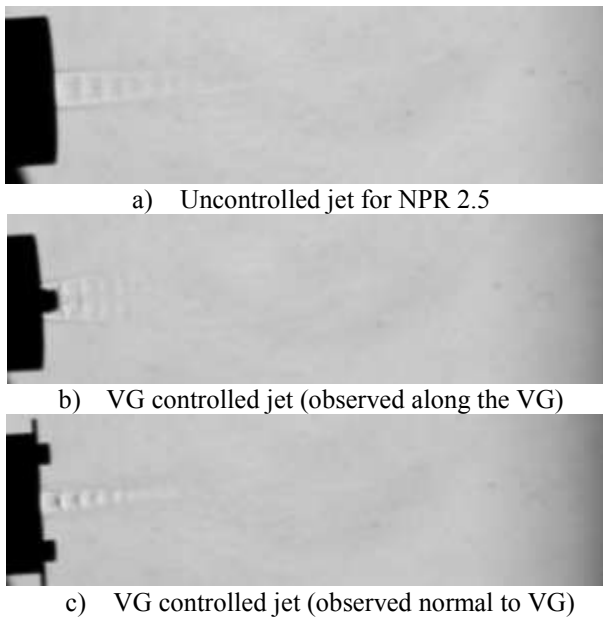

c)   VG controlled jet (observed normal to VG)

Fig. 23: Schlieren images of uncontrolled and VG controlled jets at NPR 2.5

Figure 21, Figure 22 and Figure 23 present Schlieren images capturing the stages of underexpansion, correct expansion, and overexpansion conditions corresponding to NPR 6, 4.25, and 2.5, respectively. The visualizations for the axisymmetric uncontrolled free jet reveal the presence of notable potential core length for all the expansion conditions. These images confirm that in the downstream, there is enhanced mixing. Notably, vortex generators play a significant role in improving mixing in the near field, evidenced by the presence of only one prominent shock cell observed in both directions. Besides, the introduction of vortex generators contributes to the bifurcation of the jet, responsible for enhanced mixing. These visualizations affirm that vortex generators distort the wave structure within the supersonic core. This distortion in the core is crucial for effective mixing and noise reduction, highlighting the efficacy of vortex generators in enhancing jet mixing and reducing aeroacoustic noise.

4   Conclusion

In the present study, both the experimental and the numerical investigations have been conducted for a thorough understanding of supersonic axisymmetric jets. The computational validation has been done incorporating the Rayleigh Pitot formula for the uncontrolled jet, which has not been found in any other validation studies, as per the authors' understanding. The velocity vector contour from the computational investigation reveals that there is

circulation near the jet shear layer which is responsible for the entrainment of the surrounding fluid. The eddy viscosity and the turbulent kinetic energy are substantially higher at the jet shear later in the near stream, causing a higher entrainment rate at that location. At the far stream, since the jet is spread over a significant length, eddy viscosity, and the turbulent kinetic energy are diffused over the entire region. In addition, the investigation is extended to experimentally study the effect of vortex generators on jet flow. It has been observed that the mixing efficiency is substantially improved due to the VG placed at the nozzle exit. Also, a significant reduction in the jet core length was observed, particularly in underexpanded conditions, illustrating the pivotal role of VGs in enhancing mixing efficiency under favorable pressure gradients. The introduction of VG leads to the formation of small-scale vortices which distort the shock cell structure and wave patterns of the supersonic core region. This essentially results in efficient mixing which thereby reduces jet noise. This research underscored the effectiveness of VGs in amplifying the mixing of Mach 1.6 jets, holding promise for improved jet performance in the realm of aerospace engineering.

The future scope of this research involves extending the computational analysis to account for elevated jet temperatures, which is more suitable for real-world conditions. This would enhance the understanding of the jets' behavior in diverse thermal environments, contributing to broader applications and valuable insights into the jet flow.

Nomenclature:

CD   : Convergent divergent
NPR   : Nozzle Pressure Ratio
L_c : Supersonic core length
D_h : Nozzle diameter
a   : Nozzle radius
M   : Mach number
AR   : Aspect Ratio
γ : The ratio of specific heats.
M_1 : Mach number upstream of the shock wave
De   : Exit Diameter
P   : Pitot Pressure
P_o : Settling chamber pressure
VG   : Vortex Generator

References:
[1] Decher R., Infrared emissions from turbofans with high aspect ratio nozzles, *Journal of Aircraft*, Vol. 18, No. 12, 1981, pp. 1025–1031.

[2] Brown G. L. and Roshko A., On density effects and large structure in turbulent mixing layers, *Journal of Fluid Mechanics*, Vol. 64, No. 4, 1974, pp. 775–816. https://doi.org/10.1017/S002211207400190X.

[3] Liepmann D., and Gharib M., The role of streamwise vorticity in the near-field entrainment of round jets, *Journal of Fluid Mechanics*, Vol. 245, 1992, pp. 643-668.

[4] Rahman A. A., A Review of Effects of Initial and Boundary Conditions on Turbulent Jets, *WSEAS Transactions on Fluid Mechanics*, Vol. 5, No. 4, 2010, pp. 257-275.

[5] Mohanta P. K., and Sridhar B. T. N., Effect of hydraulic diameter on potential core decay of supersonic jets, *INCAS Bulletin*, Vol. 12, 2020, pp. 119-126.

[6] Pannu S., and Johannesen N., The structure of jets from notched nozzles. *Journal of Fluid Mechanics*. 74, 1976, pp. 515 - 528.

[7] Ilakkiya S., and Sridhar B. T. N., An experimental study on the effect of square grooves on decay characteristics of a supersonic jet from a circular nozzle, *Journal of Mechanical Science and Technology*, Vol. 32, No.10, 2018, pp. 4721–4729.

[8] Balakrishnan P., and Srinivasan, K., Jet noise reduction using co-axial swirl flow with curved vanes, *Applied Acoustics*, Vol. 126, 2017, pp. 149–161.

[9] Rao S. M. V., Karthick S. K., and Anand, A., Elliptic supersonic jet morphology manipulation using sharp-tipped lobes, *Physics of Fluids*, Vol. 32. 086107, 2020. https://doi.org/10.1063/5.0015035.

[10] Li X., Experimental Investigation of Jet Flow Fields with Chevron Nozzles, *IOP Conference Series: Materials Science and Engineering*, 782(4), 2020. https://doi.org/10.1088/1757-899X/782/4/042010.

[11] Bradbury L. J. S. and Khadem A. H., The distortion of a jet by tabs. *Journal of Fluid Mechanics*, Vol. 70, No. 4, 1975, pp. 801 - 813.

[12] Ahuja K., and Brown W., Shear flow control by mechanical tabs, In *AIAA 2nd Shear Flow Conference*, 1989, pp. 1989-994.

[13] Brown W. H., and Ahuja K. K, Enhancement of Mixing in a Rectangular Jet by Mechanical Tabs. *NASA Contractor Report*, 185207, 1990.

[14] Zaman K., Samimy M., and Reeder M., Effect of tabs on the evolution of an axisymmetric jet, *NASA Technical Memorandum 104472*, 1991.

[15] Samimy M., Zaman K. B. M. Q., and Reeder M. F., Effect of tabs on the flow and noise field of an axisymmetric jet, *AIAA Journal*, Vol. 31, No. 4, 1993, pp. 609-619.

[16] Arunkumar P., Rathakrishnan E., Triangular tabs for supersonic jet mixing enhancement, *The Aeronautical Journal*, Vol. 118, 2014, pp. 1245-1278.

[17] Phanindra, B. C. and Rathakrishnan, E., Corrugated tabs for supersonic jet control, *AIAA Journal*, Vol. 48, No. 2, 2010, pp. 453–465.

[18] Jana T., Kaushik M., Performance of corrugated actuator-tabs of aspect ratio 2.0 on supersonic jet mixing enhancement, *Journal of Mechanical Science and Technology*, Vol. 35, 2021, pp. 1087–1097.

[19] Anderson J. D., Modern compressible flow: with historical perspective, *McGraw-Hill Education*, New York, 2021.

[20] Ranjan A., Kaushik M., Deb D., Muresan V., and Unguresan M., Assessment of Short Rectangular-Tab Actuation of Supersonic Jet Mixing, *Actuators*, Vol. 9, 2020. https://doi.org/10.3390/act9030072.

[21] Anderson J. D., Fundamentals of Aerodynamics, *McGraw-Hill Education*, New York, 2017.

Contribution of Individual Authors to the Creation of a Scientific Article (Ghostwriting Policy)

Paramesh T performed the experiments and wrote the first draft. Tamal Jana supervised the study and edited the manuscript. Mrinal Kaushik edited and reviewed the final draft. The authors read and approved the final manuscript.

Sources of Funding for Research Presented in a Scientific Article or Scientific Article Itself

No funding was received for conducting this study.

Conflict of Interest

The authors have no conflicts of interest to declare.

Creative Commons Attribution License 4.0 (Attribution 4.0 International, CC BY 4.0)